

Fluctuations as probe of the QCD phase transition and freeze-out in heavy ion collisions at LHC and RHIC

B. Friman¹, F. Karsch^{2,3}, K. Redlich^{4,5} and V. Skokov¹

¹ GSI Helmholtzzentrum für Schwerionenforschung, D-64291 Darmstadt, Germany,

² Fakultät für Physik, Universität Bielefeld, D-33501 Bielefeld, Germany

³ Physics Department, Brookhaven National Laboratory, Upton, NY 11973, USA

⁴ Institute of Theoretical Physics University of Wrocław, PL-50204 Wrocław, Poland

⁵ ExtreMe Matter Institute EMMI, GSI, D-64291 Darmstadt, Germany

Abstract

We discuss the relevance of higher order cumulants of net baryon number fluctuations for the analysis of freeze-out and critical conditions in heavy ion collisions at LHC and RHIC. Using properties of $O(4)$ scaling functions, we discuss the generic structure of these higher cumulants at vanishing baryon chemical potential and apply chiral model calculations to explore their properties at non-zero baryon chemical potential. We show that the ratios of the sixth to second and eighth to second order cumulants of the net baryon number fluctuations change rapidly in the transition region of the QCD phase diagram. Already at vanishing baryon chemical potential they deviate considerably from the predictions of the hadron resonance gas model which reproduce the second to fourth order cumulants of the net proton number fluctuations at RHIC. We point out that the sixth order cumulants of baryon number and electric charge fluctuations remain negative at the chiral transition temperature. Thus, they offer the possibility to probe the proximity of the chemical freeze-out to the crossover line.

1 Introduction

Strongly interacting matter at high temperature or large net baryon number density is expected to undergo a rapid transition from a phase with hadrons as dominant degrees of freedom to a phase where partonic degrees of freedom prevail. At vanishing baryon chemical potential ($\mu_B = 0$), this transition is a true second order phase transition only in the limit of vanishing light quark masses. For $\mu_B > 0$, however, a second order phase transition point, the so-called chiral critical point, may exist also for physical values of the quark masses. A large experimental as well as theoretical effort is put into the exploration of the QCD phase transitions and the development of appropriate tools and observables that can provide a univocal signal for the existence of the phase transitions and their universal properties. The analysis of fluctuations of various physical observables [1], in particular of the net baryon number, may serve this purpose [2, 3]. Theoretically, the properties of the corresponding susceptibilities are well understood at high temperature (T) and small values of the baryon chemical potential (μ_B). In this regime, they are suitable observables for localizing the phase boundary in the μ_B - T plane.

Critical behavior is signaled by long range correlations and increased fluctuations, owing to the appearance of massless modes at a second order phase transition. Fluctuations of baryon number and electric charge have been shown to be sensitive indicators for such critical behavior [4]. In the exploration of the QCD phase diagram at non-zero temperature and baryon chemical potential, higher order cumulants of baryon number fluctuations play a particularly important role. They diverge on the chiral phase transition line $T_c(\mu_B, m_q \equiv 0)$ as well as at the elusive chiral critical point [5].

In heavy ion experiments, a lot of information has been collected on particle yields in a wide range of beam energies [6]. The particle multiplicities are well described in a thermal model using the partition function of a hadron resonance gas (HRG) [7]. Ratios of particle yields at a given beam energy can be characterized by a few thermal parameters, e.g. temperature and chemical potentials for baryon number, electric charge and strangeness. These parameters define the freeze-out conditions, *i.e.* the thermal parameters corresponding to the last interaction of the hadrons participating in the collective expansion and cooling of the hot and dense matter formed in a heavy ion collision. Data obtained at small values of the baryon chemical potential suggest that the freeze-out curve $T_f(\mu_B)$ is close to the expected QCD phase boundary. In particular, at $\mu_B = 0$ the chemical freeze-out seems

to occur at or very near the QCD transition region for a physical quark mass spectrum [8]. At larger values of μ_B/T , however, there is a discrepancy between the slope of the freeze-out curve and current lattice QCD results on the curvature of the chiral phase transition line [9].

The HRG model, which is based on the observed hadron spectrum, does not exhibit critical behavior nor does it reflect the sudden change of degrees of freedom in the transition to the partonic phase of QCD. In the chiral limit, close to the phase transition line $T_c(\mu_B, m_q \equiv 0)$ fluctuations of e.g. the net baryon number density are expected to reflect the universal properties [10] of the 3-dimensional, $O(4)$ symmetric spin model [11]. The $O(4)$ scaling relations for cumulants of net baryon number fluctuations differ significantly from predictions based on the HRG model. Lattice calculations of cumulants of baryon number and electric charge fluctuations, performed in the transition region at vanishing baryon chemical potential and non-zero quark mass, do indeed show that these cumulants differ qualitatively from those of the HRG model and reflect the basic feature expected close to the chiral phase transition [4]. This suggests that at physical values of the light and strange quark masses these cumulants are sensitive to the critical dynamics in the chiral limit and may be employed to characterize also the crossover transition in strongly interacting matter.

Thus, also at vanishing baryon chemical potential, *i.e.* under the conditions approximately realized in the high energy runs at RHIC or LHC, the question arises to what extent a refined analysis of the freeze-out conditions can establish the existence of the chiral phase transition. At $\mu_B/T \simeq 0$, net quark number fluctuations and their higher cumulants can be computed within the framework of lattice QCD [4, 12]. Such calculations will eventually provide a complete theoretical characterization of the thermal conditions in the crossover region. This may then be used to unravel the relation of the freeze-out conditions at RHIC and LHC energies to the pseudo-critical line in the QCD phase diagram, provided the system remains close to thermal equilibrium during freeze-out. At present, however, lattice calculations provide only limited information on cumulants up to eighth order. In particular, controlled predictions on their properties in the continuum limit are still lacking; their characteristic features are obtained on a qualitative level, but quantitative results are not yet available. Viable alternatives for discussing qualitative features of the net baryon number fluctuations is offered by $O(4)$ scaling theory and by chiral models, like e.g. the Nambu-Jona-Lasinio (NJL) model. In particular, the effective models have the advantage that they can

be extended to $\mu_B > 0$ with minimal effort. On the other hand, a clear disadvantage of NJL-type chiral models is that they do not account for the potentially large contribution from resonances in the hadronic phase.

In this paper we will discuss the robust features of cumulants of net baryon number fluctuations that can be extracted from considerations based on $O(4)$ universality, on existing lattice calculations and on model calculations. In the next section we discuss higher order cumulants at vanishing baryon chemical potential making use mainly of $O(4)$ universality. In Section 3 we extend these considerations to $\mu_B/T > 0$ using results from model calculations. In Section 4 we summarize the relevance of our findings for experimental studies of baryon number fluctuations at LHC and RHIC and in Section 5 we give our conclusions.

2 Charge fluctuations at $\mu_B = 0$

2.1 $O(4)$ scaling functions and net baryon number fluctuations

Close to the chiral limit and at temperatures near the chiral phase transition temperature T_c , higher order derivatives of the free energy density (f) with respect to temperature or chemical potential are increasingly sensitive to the non-analytic (singular) part (f_s). We may represent the free energy density in terms of the singular and regular contributions

$$f(T, \mu_q, m_q) = f_s(T, \mu_q, m_q) + f_r(T, \mu_q, m_q). \quad (1)$$

In addition to the dependence on temperature T , we also introduce here an explicit dependence on the light quark chemical potential, $\mu_q = \mu_B/3$, and the (degenerate) light quark masses $m_q \equiv m_u = m_d$. For simplicity we do not take the chemical potentials for electric charge and strangeness into account, nor do we introduce an explicit dependence on the strange quark mass. The singular part of the free energy may be written as

$$\frac{f_s(T, \mu_q, h)}{T^4} = Ah^{1+1/\delta} f_f(z), \quad z \equiv t/h^{1/\beta\delta}, \quad (2)$$

where β and δ are critical exponents of the 3-dimensional $O(4)$ spin model [11] and

$$\begin{aligned} t &\equiv \frac{1}{t_0} \left(\frac{T - T_c}{T_c} + \kappa_q \left(\frac{\mu_q}{T} \right)^2 \right), \\ h &\equiv \frac{1}{h_0} \frac{m_q}{T_c}. \end{aligned} \quad (3)$$

Here T_c is the critical temperature in the chiral limit and t_0, h_0 are non-universal scale parameters (as is T_c). We use the chiral transition temperature T_c also to set the scale for the explicit symmetry breaking, introduced by the non-vanishing light quark masses¹. The amplitude A is fixed by the relation of the scaling function for the free energy density, $f_f(z)$, to the more commonly used scaling function $f_G(z)$, which characterizes the scaling properties of the chiral condensate, or in general the order parameter (M) in $O(4)$ symmetric models, $M = h^{1/\delta} f_G(z)$, where

$$f_G(z) = - \left(1 + \frac{1}{\delta} \right) f_f(z) + \frac{z}{\beta\delta} f'_f(z). \quad (4)$$

The scaling function $f_f(z)$ and its derivatives $f_f^{(n)}(z)$ have recently been determined for $n \leq 3$ using high precision Monte Carlo simulations of the 3-dimensional $O(4)$ spin model and the known asymptotic series expansions [16]. We will use these results as a starting point for a discussion of the generic structure of higher order cumulants of the net baryon number fluctuations.

Note that the reduced temperature t , introduced in Eq. (3), depends explicitly on the quark chemical potential. The constant $\kappa_q \simeq 0.06$, which controls the curvature of the chiral phase boundary for small values of μ_q/T , was recently determined in a scaling analysis of (2+1)-flavor QCD [9]. A comparison with other lattice results for κ_q [17, 18], suggests that this parameter is only weakly dependent on the quark mass and the number of flavors.

In this paper we focus on the properties of the net baryon number fluctuations. The corresponding cumulants are obtained from Eq. (1) by taking derivatives with respect to $\hat{\mu}_q = \mu_q/T$,

$$\chi_n^B = - \frac{1}{3^n} \frac{\partial^n f/T^4}{\partial \hat{\mu}_q^n}. \quad (5)$$

¹In Ref. [15] the strange quark mass was used to set the scale for the symmetry breaking term.

From Eq. (2) it is apparent that, in the vicinity of the critical temperature, the susceptibilities χ_n^B show a strong dependence on the explicit symmetry breaking term, the quark mass,

$$\chi_n^B \sim \begin{cases} -(2\kappa_q)^{n/2} h^{(2-\alpha-n/2)/\beta\delta} f_f^{(n/2)}(z) & , \text{ for } \mu_q/T = 0, \text{ and } n \text{ even} \\ -(2\kappa_q)^n \left(\frac{\mu_q}{T}\right)^n h^{(2-\alpha-n)/\beta\delta} f_f^{(n)}(z) & , \text{ for } \mu_q/T > 0 \end{cases} \quad (6)$$

where we used the scaling relation $2 - \alpha = \beta\delta(1 + 1/\delta)$. Because α is negative in the 3-dimensional $O(4)$ universality class ($\alpha = -0.2131(34)$ [11]), the specific heat, or equivalently the fourth order cumulants of the net baryon number fluctuations, does not diverge at the chiral transition temperature, *i.e.* at $z = 0$, in the chiral limit. At $\mu_q/T = 0$ the first divergent cumulant is obtained for $n = 6$, while at $\mu_q/T > 0$ this happens already for $n = 3$. We note that the singular structure appearing in n -th order cumulants for $\mu_q/T > 0$ is identical to that of $(2n)$ -th order cumulants at $\mu_q/T = 0$, since the chemical potential enters quadratically in the reduced temperature t . This characteristic has been used in Refs. [13, 14] to exploit properties of third order cumulants at non-zero baryon chemical potential as signatures for critical behavior. In this case, however, the singular contributions are suppressed by a factor $(\mu_q/T)^{n/2}$ relative to the sixth order cumulants at $\mu_q/T = 0$. Consequently, in the mean-field analysis of Ref. [13], it was found that qualitative changes of the third-order cumulant, e.g. a change of sign in χ_3^B , is found only at rather large values of the chemical potential, $\mu_B/T > 4$.

Using Eq. (6), one finds the leading singularity in the chiral limit,

$$\chi_n^B \sim \begin{cases} -(2\kappa_q)^{n/2} |t|^{2-\alpha-n/2} f_{\pm}^{(n/2)} & , \text{ for } \mu_q/T = 0, \text{ and } n \text{ even} \\ -(2\kappa_q)^n \left(\frac{\mu_q}{T}\right)^n |t|^{2-\alpha-n} f_{\pm}^{(n)} & , \text{ for } \mu_q/T > 0, \end{cases} \quad (7)$$

where

$$f_{\pm}^{(n)} = \lim_{z \rightarrow \pm\infty} |z|^{-(2-\alpha-n)} f_f^{(n)}(z). \quad (8)$$

The singular part of χ_4^B , which is proportional to $f_f^{(2)}$, has the same singular structure as the specific heat; it is proportional to the second derivative of the free energy with respect to temperature. Thus, using the convention of Ref. [19], we may write $\chi_4^B(t)$ in the chiral limit at $\mu_q/T = 0$,

$$\chi_4^B(t) \sim \chi_r + \frac{A^{\pm}}{\alpha} |t|^{-\alpha}, \quad (9)$$

where A^+ is the amplitude above and A^- below the critical temperature. The amplitudes A^\pm are positive and the ratio $A^+/A^- \simeq 1.8$. This implies that the cumulants $\chi_n^B(t)$ are positive for all $n > 4$ and $t < 0$, while for $t > 0$ they alternate in sign. At non-zero values of the quark mass, $h > 0$, we thus expect χ_6^B to change sign in the transition region and χ_8^B to do so twice. For a given $h > 0$, this is reflected in the z -dependence of the scaling functions $f_f^{(n)}(z)$, as shown² in Figs. 1 and 2. In fact, the temperature and quark mass dependence of the singular parts of the net baryon number fluctuations is directly related to the scaling functions $f_f^{(n)}(z)$ of the 3-dimensional $O(4)$ model [16]. Thus, the generic structure of the fourth and sixth order cumulants can be obtained from the known $O(4)$ scaling functions, in the chiral limit as well as for non-zero values of the quark mass.

In the chiral limit, the non-analytic contribution to χ_4^B vanishes at the chiral transition temperature, $t = 0$. Consequently, in the transition region, the regular terms dominate in χ_4^B . Nonetheless, the non-analytic term in χ_4^B varies rapidly with temperature, leading to a pronounced maximum in the transition region, observed in lattice as well as model calculations.

The temperature at which χ_6^B changes sign is non-universal since it depends on the magnitude of the regular terms. However, in the scaling regime the location of the extrema and the corresponding amplitudes follow universal scaling laws. Moreover, we note that the positions of the two extrema of $f_f^{(3)}(z)$, $z^- < 0$ and $z^+ > 0$, provide bounds on the critical temperature in the chiral limit.

It is evident from Figs. 1 and 2 that the $O(4)$ scaling functions show much more structure and a stronger quark mass dependence in the symmetric phase, $t > 0$, than in the broken phase, $t < 0$. In the latter case, the divergence at $t = 0$ builds up much more slowly than on the high temperature side. The scaling function $f_f^{(3)}(z)$ changes sign close to $z = 0$, while $f_f^{(4)}(z)$ does so already at $z^- < 0$. Furthermore, we note that the position of the maximum of $f_f^{(3)}(z)$ is at $z^+ \simeq 1.45$ [16], which is close to the peak position

² From the result for $f_f^{(3)}(z)$ [16] we also constructed an estimate for the next derivative, $f_f^{(4)}(z)$, which required some smoothening of the interpolations that entered the determination of $f_f^{(3)}(z)$. The resulting scaling function and the resulting quark mass dependence of $\chi_8^B(t)$ is shown in Fig. 2. We want to use it here to point out the qualitative structure that does arise within the $O(4)$ universality class, but do not consider this figure as being correct on the quantitative level, *i.e.* as far as the accurate location of the minima and the height of peaks is concerned.

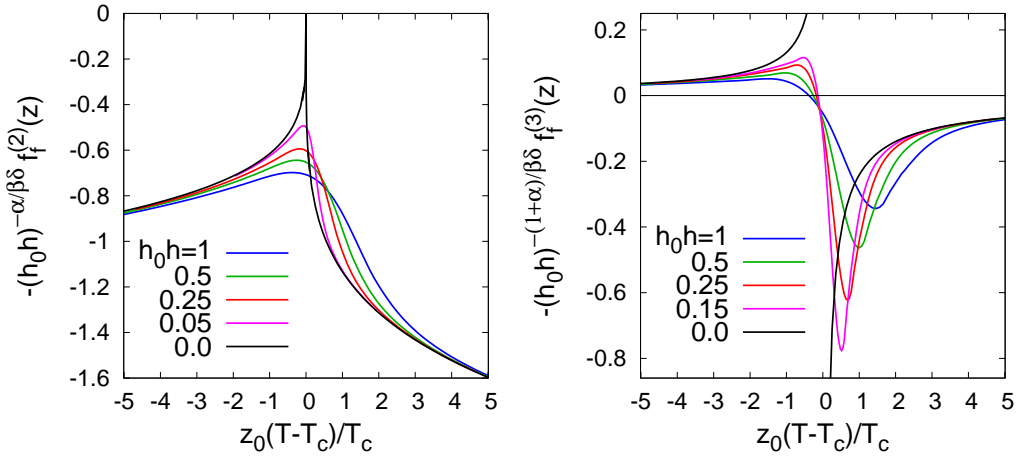


Figure 1: Scaling of the non-analytic contributions to χ_4^B (left) and χ_6^B (right) arising from second and third derivatives of the singular part of the free energy. Shown are results for different values of the symmetry breaking parameter $h_0 h = m_q/T_c$; h_0 and $z_0 = h_0^{1/\beta\delta}/t_0$ are non-universal scale parameters. Note that for $h_0 h = 1$ the abscissa is the scaling variable z . The corresponding curve thus directly shows the $O(4)$ scaling function.

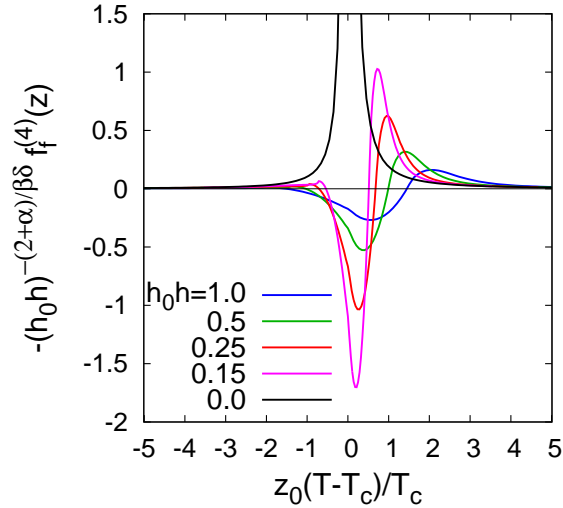


Figure 2: Same as Fig. 1 but for the non-analytic contributions to χ_8^B .

of the chiral susceptibility, $z_p \simeq 1.33(5)$ [11]. The location of these extrema define pseudo-critical temperatures $T_{6\pm}$, which converge to that of the second order chiral phase transition temperature T_c in the chiral limit,

$$\frac{T_{6\pm}(m_q)}{T_c} = 1 + \frac{z^\pm}{z_0} \left(\frac{m_q}{T_c} \right)^{1/\beta\delta}, \quad (10)$$

where $1/\beta\delta \simeq 0.55$. The proportionality constant z_0 is uniquely determined in the scaling regime of QCD with two light quarks [15] and is the same constant, which also controls the scaling of the pseudo-critical temperature T_χ determined from the position of the peak in the chiral susceptibility,

$$\frac{T_\chi(m_q)}{T_c} = 1 + \frac{z_p}{z_0} \left(\frac{m_q}{T_c} \right)^{1/\beta\delta}. \quad (11)$$

With decreasing quark mass the minimum of χ_6^B decreases as,

$$\chi_{6,min}^B \sim - \left(\frac{m_q}{T_c} \right)^{-(1+\alpha)/\beta\delta} \simeq - \left(\frac{m_q}{T_c} \right)^{-0.66}. \quad (12)$$

We also note that corrections to $\chi_{6,min}^B$ at non-zero μ_q/T start at $\mathcal{O}((\mu_q/T)^4)$. We thus expect that the basic structure of higher cumulants persists also for $\mu_B/T > 0$.

2.2 Sixth order cumulant and the QCD transition temperature

Based on the generic structure of the $O(4)$ scaling functions we thus can understand the basic features of the temperature dependence of higher cumulants of the baryon number fluctuations at vanishing baryon chemical potential. We focus on the properties of the sixth order cumulant, $\chi_6^B(T)$, or correspondingly the ratio of cumulants $R_{6,2}^B(T) = \chi_6^B(T)/\chi_2^B(T)$. In the hadronic phase, $\chi_6^B(T)$ first grows with increasing temperature. It exhibits a maximum in the hadronic phase, close to the transition region and then drops rapidly. In the entire high temperature regime, $\chi_6^B(T)$ and consequently $R_{6,2}^B(T)$ remain negative. Lattice calculations of $\chi_6^B(T)$ [10, 20] suggest that in QCD with physical quark masses, these basic features, which are due to the singular terms in χ_n^B , persist. In particular, $\chi_6^B(T) < 0$ in the vicinity of the pseudo-critical temperature for chiral symmetry restoration.

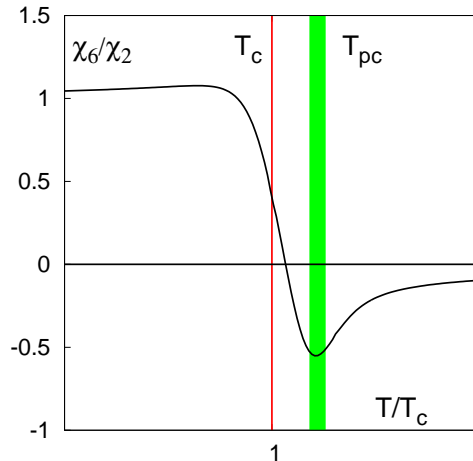


Figure 3: Schematic plot of the temperature dependence of the ratio of the sixth and second order cumulants of the net baryon number fluctuations in units of the phase transition temperature T_c in the chiral limit. The vertical lines show the chiral phase transition temperature and the pseudo-critical temperature T_{pc} , corresponding to a peak in the chiral susceptibility in QCD with physical light quark masses.

We thus expect the sixth order cumulant to be a very sensitive probe for the temperature at which the freeze-out of hadrons in heavy ion collisions occurs. In fact, it is conceivable that hadronic freeze-out occurs in a temperature regime above the QCD phase transition temperature in the chiral limit, *i.e.* it may occur close to the pseudo-critical temperature that signals the onset of chiral symmetry restoration. In that case we would expect to observe

$$R_{6,2}^B(T) \equiv \frac{\chi_6^B(T)}{\chi_2^B(T)} < 0 \text{ at freeze-out at LHC and RHIC high energy runs.}$$

This would be in striking contrast to conventional HRG model calculations, which predict $R_{6,2}^B = 1$. A similar conclusion can be drawn for the eighth order cumulant χ_8^B or, equivalently, the ratio $R_{8,2}^B$.

In more general terms we suggest that a determination of $R_{6,2}^B$ at large collision energies at RHIC or LHC will provide a characteristic signature for the location of the freeze-out temperature relative to the QCD phase transition. This is illustrated in Fig. 3, where we show a schematic plot of $R_{6,2}^B$ along with the critical temperature in the chiral limit (T_c) and the crossover temperature for chiral symmetry restoration for physical light quark masses (T_{pc}).

In the following we extend the above considerations to the case of non-vanishing baryon chemical potential. We do this in the framework of a chiral model, analyzing the critical behavior of the Polyakov loop extended quark meson (PQM) model in the functional renormalization group approach [14]. This allows us to compute the dependence of higher cumulants on μ_q/T and T . We determine the line of minima of $R_{6,2}^B$ in the μ_q - T plane and compare this with the chiral transition line as well as with the pseudo-critical line obtained at a physical pion mass.

3 Higher cumulants of charge fluctuations at $\mu_B/T > 0$

The universal features of the 3-dimensional $O(4)$ scaling functions discussed in the previous section also are reflected in effective chiral model calculations where the Polyakov loop is coupled to the fermion sector, thus generating many of the characteristics of the confinement-deconfinement transition [21, 22, 23, 24]. The Polyakov loop extended quark meson (PQM) model [25] is one variant. It shares with QCD a global $O(4)$ symmetry, which is spontaneously broken at low and restored at high temperatures. Thus, in the light quark mass limit, this model reproduces the universal scaling functions, discussed in the previous section. We use the PQM model to implement the basic features of the transition from hadronic matter to a quark gluon plasma into the temperature dependence of the cumulants of net baryon number fluctuations and to analyze their properties also at $\mu_q/T > 0$.

The Lagrangian of the PQM model [25],

$$\begin{aligned} \mathcal{L} = & \bar{q} [i\gamma_\mu D^\mu - g(\sigma + i\gamma_5 \vec{\tau} \vec{\pi})] q + \frac{1}{2}(\partial_\mu \sigma)^2 + \frac{1}{2}(\partial_\mu \vec{\pi})^2 \\ & - U(\sigma, \vec{\pi}) - \mathcal{U}(\ell, \ell^*) , \end{aligned} \quad (13)$$

involves interactions of mesons and gluons with fermionic fields. The coupling between the effective gluon field and quarks is implemented through the covariant derivative

$$D_\mu = \partial_\mu - iA_\mu, \quad (14)$$

where $A_\mu = g_s A_\mu^a \lambda^a/2$ and the spatial components of the gluon field are neglected, i.e. $A_\mu = \delta_{\mu 0} A_0$.

The purely mesonic potential of the model,

$$U(\sigma, \vec{\pi}) = \frac{\lambda}{4} (\sigma^2 + \vec{\pi}^2 - v^2)^2 - c\sigma, \quad (15)$$

contains a term linear in the σ field, which explicitly breaks the chiral symmetry and is used to reproduce the physical pion mass.

The effective potential for the gluon field is expressed in terms of the thermal expectation values of the color trace of the Polyakov loop and its conjugate,

$$\frac{\mathcal{U}(\ell, \ell^*)}{T^4} = -\frac{b_2(T)}{2} \ell^* \ell - \frac{b_3}{6} (\ell^3 + \ell^{*3}) + \frac{b_4}{4} (\ell^* \ell)^2 \quad (16)$$

where

$$\ell = \frac{1}{N_c} \langle \text{Tr}_c L(\vec{x}) \rangle, \quad \ell^* = \frac{1}{N_c} \langle \text{Tr}_c L^\dagger(\vec{x}) \rangle, \quad (17)$$

and

$$L(\vec{x}) = \mathcal{P} \exp \left[i \int_0^\beta d\tau A_4(\vec{x}, \tau) \right]. \quad (18)$$

Here \mathcal{P} stands for the path ordering, $\beta = 1/T$ and $A_4 = i A_0$. The potential $\mathcal{U}(\ell, \ell^*)$ preserves the $Z(3)$ symmetry of the gluonic sector of QCD.

In the Appendix, we give further details on the choice of parameters for the Polyakov loop potential and present the relevant calculational steps within the functional renormalization group (FRG) approach [26, 27, 28, 29]. Within this formalism we compute the free energy density of the PQM model [14, 30],

$$f_{\text{PQM}}(\ell, \ell^*; T, \mu) \equiv \Omega(\ell, \ell^*; T, \mu) = -\frac{T}{V} \ln Z(\ell, \ell^*; T, \mu), \quad (19)$$

as a function of temperature, chemical potential as well as the Polyakov loop variables, ℓ and ℓ^* . The latter two are then fixed by the stationarity condition:

$$\frac{\partial}{\partial \ell} \Omega(\ell, \ell^*; T, \mu) = 0, \quad \frac{\partial}{\partial \ell^*} \Omega(\ell, \ell^*; T, \mu) = 0. \quad (20)$$

The cumulants of the net baryon number fluctuations are obtained by taking suitable derivatives of the free energy, as specified in Eq. (5). In practice

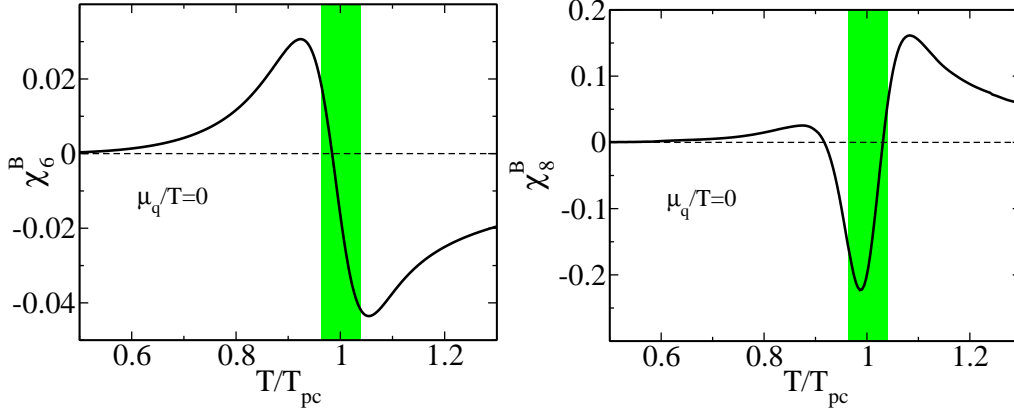


Figure 4: The sixth and eighth order cumulants of the net baryon number fluctuations at $\mu_q/T = 0$ in the PQM model. The temperature is given in units of the pseudo-critical temperature $T_{pc}(m_\pi)$ corresponding to a maximum of the the chiral susceptibility. The shaded area indicates the chiral crossover region.

these derivatives have been implemented directly into the analysis of the flow equations (see Appendix).

In Fig. 4 we show the sixth and eighth order cumulants of the net baryon number fluctuations computed at $\mu_q/T = 0$ within the PQM model for physical values of the pion mass. The basic features dictated by $O(4)$ symmetry restoration, as discussed in the previous sections, are readily identified in the figure. Moreover, the positions of the two extrema of χ_6^B correspond approximately to the zeros of χ_8^B . This confirms that in the transition region, two derivatives with respect to μ_q/T are indeed equivalent to one derivative with respect to T .

From these calculations, as well as from calculations of the lower order cumulants χ_2^B and χ_4^B , we obtain the ratios $R_{n,m}^B$ of the n -th and m -th cumulants. Results obtained for $\mu_q/T = 0$ and $\mu_q/T > 0$ are shown in Figs. 5 and 6, respectively. We note that these ratios approach unity at low temperatures, as it is the case also in the hadron resonance gas model. In the transition region, they reflect the expected $O(4)$ scaling properties; they have a shallow maximum close to the transition region before they drop sharply. In particular, they show pronounced minima with $R_{n,2}^B < 0$ in the vicinity of the chiral crossover temperature. The exact location of these minima and

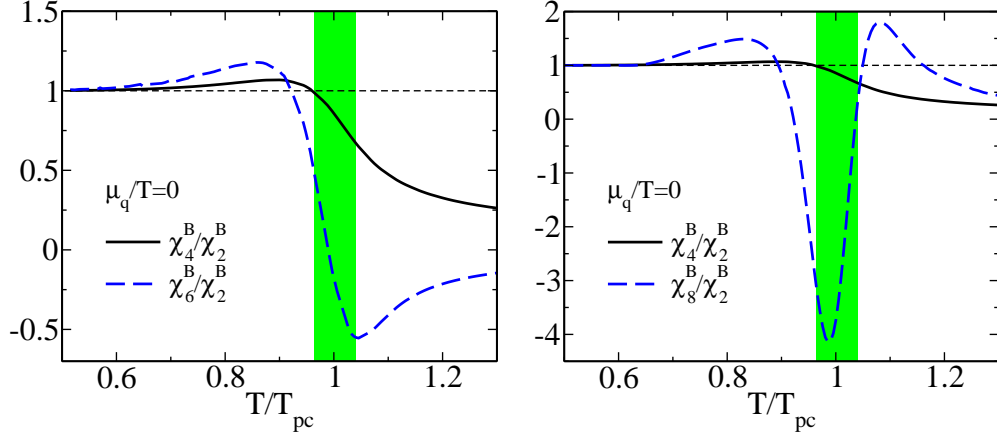


Figure 5: The temperature dependence of the fourth, sixth and eighth order cumulants of the net baryon number fluctuations χ_n^B relative to the second order one. The temperature is given in units of the chiral crossover temperature. The shaded area indicates the region of the chiral crossover transition at $\mu_q/T = 0$. The calculations were done in the PQM model within the FRG approach.

their depth is to some extent model dependent. However, we note, that in the transition region the second order cumulant used in these ratios for normalization is dominated by non-singular contributions which are positive. The minima in $R_{n,2}^B$ therefore mainly reflect the strong temperature dependence of higher cumulants χ_n^B . We also note that these minima become more pronounced with increasing μ_q/T . In fact, the structure of e.g. $R_{6,2}^B$ becomes similar to that of χ_8^B at large μ_q/T . This is easily understood in terms of the Taylor expansion of $R_{6,2}^B$, where the dominant correction at non-zero μ_q/T is due to χ_8^B ,

$$\begin{aligned}
 R_{6,2}^B(\mu_q/T) &= R_{6,2}^B(0) + \frac{1}{2} \left(\frac{\mu_q}{T} \right)^2 (R_{8,2}^B(0) - R_{6,2}^B(0)R_{4,2}^B(0)) \\
 &\quad + \mathcal{O}((\mu_q/T)^4).
 \end{aligned}
 \tag{21}$$

This also makes it clear why for $\mu_q/T > 0$ the location of the minimum of $R_{6,2}^B(\mu_q/T)$ is shifted to lower temperatures relative to that of the chiral crossover temperature. Similarly, at non-zero μ_q/T , the ratio $R_{8,2}^B(\mu_q/T)$ shows more pronounced oscillations in the transition region, due to contributions from higher order cumulants, which oscillate more rapidly in the

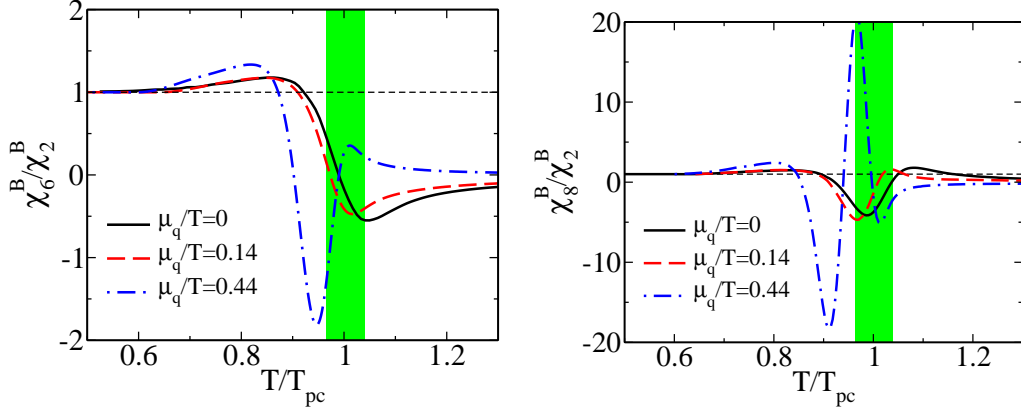


Figure 6: Comparison of the temperature dependence of the ratios χ_6^B/χ_2^B and χ_8^B/χ_2^B for various μ_q/T corresponding to values at chemical freeze-out in heavy ion collisions at RHIC. The shaded area indicates the region of the chiral crossover transition at $\mu_q/T = 0$.

transition region. The amplitude of the maximum at high temperatures becomes compatible in magnitude with that of the minimum.

4 Freeze-out and the QCD transition

The analysis of universal scaling functions that control the thermodynamics in the vicinity of a phase transition in the universality class of 3-dimensional $O(4)$ symmetric theories (section 2), of model (section 3) and of lattice calculations [20, 33] suggest that at vanishing baryon chemical potential the sixth order cumulant of the net baryon number fluctuations is negative in the entire high temperature phase. In fact, the $O(4)$ scaling functions for higher cumulants turn negative already in the vicinity of the chiral ($m_q = 0$) critical temperature, *i.e.* below the crossover temperature ($m_q > 0$), which is relevant for the transition at non-zero values of the light quark masses. The regular terms in the QCD free energy may shift the onset of the negative regime to higher temperatures. However, model [32] as well as lattice [20, 33] calculations suggest that the regime of negative sixth order cumulants starts below but close to the QCD crossover transition temperature.

At non-zero baryon chemical potential, the temperature interval of nega-

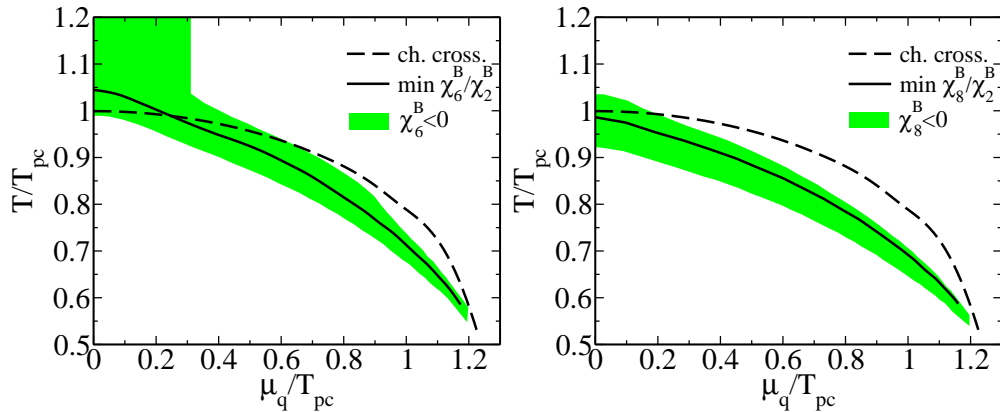


Figure 7: The chiral crossover line [dashed line] and the first minima in χ_6^B (left) and χ_8^B (right) [solid line]. The bands show the parameter range for which χ_6^B and χ_8^B , respectively, are negative in the neighborhood of these minima.

time χ_6^B , or equivalently $R_{6,2}^B(\mu_q/T)$, shrinks and follows the crossover transition line. This is illustrated in Fig. 7, which shows the temperature interval, closest to the hadronic phase, where the sixth and eighth order cumulants of the net baryon number fluctuations are negative, as obtained in the FRG approach to the PQM model. It is evident that the sixth order cumulant χ_6^B is negative in a wide range of temperatures which extends into the symmetry broken phase. This is even more the case for the eighth order cumulant as expected from the structure of the corresponding $O(4)$ scaling function. Except for a small range of chemical potential values close to $\mu_q/T = 0$, the eighth order cumulant is, however, positive again on the crossover line.

5 Discussion and Conclusions

We have shown that higher order cumulants of the net baryon number fluctuations are sensitive probes for the analysis of freeze-out conditions in heavy ion collisions and may allow to clarify their relation to the QCD phase transition. This is the case at LHC energies as well as at the entire regime of beam energies covered by the low energy run at RHIC. If in heavy ion collisions, particles are produced from a thermalized system, the analysis of higher cu-

mulants of the net baryon number fluctuations does provide constraints on the location of the freeze-out temperature relative to the chiral transition temperature. We find that the most robust statements, which become rigorous in the chiral limit, can be made for the sixth order cumulants of charge fluctuations for small values of the quark chemical potential:

If freeze-out occurs close to the chiral crossover temperature the sixth order cumulant of the net baryon number fluctuations will be negative at LHC energies as well as for RHIC beam energies $\sqrt{s_{NN}} \gtrsim 60$ GeV, corresponding to $\mu_B/T \lesssim 0.5$. This is in contrast to hadron resonance gas model calculations which yield a positive sixth order cumulant.

We also note that the basic features discussed here for net baryon number fluctuations also carry over one-to-one to electric charge fluctuations. In the chiral limit, the most singular component in the cumulants of electric charge fluctuations is proportional to the singular part of the corresponding cumulant of net baryon number fluctuations. In fact, lattice [33] and model [34] calculations of the sixth order cumulant of electric charge fluctuations at $\mu_q/T = 0$ show that this cumulant is negative in the high temperature phase of QCD. The ratio of the sixth and second order cumulants, χ_6^Q/χ_2^Q rapidly drops in the transition region from the HRG value $(\chi_6^Q/\chi_2^Q)_{HRG} \simeq 10$ to about -4 at the chiral crossover temperature. Also this ratio is therefore a sensitive probe of the conditions at freeze-out and their relation to the critical behavior in strongly interacting matter.

We finally comment on the fourth order cumulants, in particular on the ratio χ_4^B/χ_2^B recently measured by STAR [35] as well as the corresponding ratio for cumulants for electric charge fluctuations, χ_4^Q/χ_2^Q . The former is consistent with the HRG value $(\chi_4^B/\chi_2^B)_{HRG} = 1$ [36, 37]. If freeze-out occurs in the hadronic phase, one expects to find also large values for ratios of cumulants of electric charge fluctuations, $(\chi_4^Q/\chi_2^Q)_{HRG} \simeq 1.8$ [36]. On the other hand, if freeze-out occurs at the crossover temperature, also these ratios will deviate from the HRG values. Lattice calculations suggests that both ratios drop rapidly in the transition region, but stay positive also in the high temperature phase [33].

In Table 1 we summarize two different freeze-out scenarios characterized by various ratios of the cumulants of the net baryon number and electric charge fluctuations, respectively. These scenarios assume that in heavy ion collisions the freeze-out of hadrons occurs from a thermalized system characterized by the phenomenologically determined freeze-out curve $T_f(\mu_B^f)$. Ta-

freeze-out conditions	χ_4^B/χ_2^B	χ_6^B/χ_2^B	χ_4^Q/χ_2^Q	χ_6^Q/χ_2^Q
HRG	1	1	~ 2	~ 10
QCD: $T^{freeze}/T_{pc} \lesssim 0.9$	$\gtrsim 1$	$\gtrsim 1$	~ 2	~ 10
QCD: $T^{freeze}/T_{pc} \simeq 1$	~ 0.5	< 0	~ 1	< 0

Table 1: Values for ratios of cumulants of net baryon number (B) and electric charge (Q) fluctuations for the case that freeze-out appears well in the hadronic phase (third row) or in the vicinity of the chiral crossover temperature (fourth row). We give results based on current lattice calculations [20, 33] and on the calculations presented here. In the second row we give results of a HRG model calculation [33]. We also note that unlike the cumulants of net baryon number fluctuations the ratios of cumulants of electric charge fluctuations vary somewhat as a function of the baryon chemical potential along the freeze-out line.

ble 1 shows, that ratios of cumulants of charge fluctuations are very sensitive to possible differences in freeze-out and crossover temperature. Finally, we note that these results do not account for possible finite volume effects nor for possible effects of the evolution from chemical towards thermal freeze-out in heavy ion collisions.

Acknowledgments

We gratefully acknowledge discussions with Jürgen Engels on the $O(4)$ scaling functions. The work of F.K. was supported in part by contract DE-AC02-98CH10886 with the U.S. Department of Energy, by the BMBF under grant 06BI401 and the GSI Helmholtzzentrum für Schwerionenforschung under grant BILAER. K.R. acknowledges partial support by the Polish Ministry of Science (MEN). B.F. and K.R. were supported in part by the ExtreMe Matter Institute (EMMI). V.S. acknowledges support by the Frankfurt Institute for Advanced Studies (FIAS).

Appendix

Here we summarize the basic steps involved in the calculation of the free energy of the PQM model within the functional renormalization group (FRG)

approach. We also describe the methods used to obtain the FRG results for the cumulants of the net baryon number fluctuations. Further details on these calculations are given in Refs. [30, 14, 31].

In the PQM model Lagrangian introduced in Eqs. (13-18), we need to specify the parameters used in the Polyakov loop potential (16). These parameters were chosen to reproduce the equation of state of pure $SU(3)$ lattice gauge theory,

$$b_2(T) = a_0 + a_1 \left(\frac{T_0}{T}\right) + a_2 \left(\frac{T_0}{T}\right)^2 + a_3 \left(\frac{T_0}{T}\right)^3, \quad (22)$$

with $a_0 = 6.75$, $a_1 = -1.95$, $a_2 = 2.625$, $a_3 = -7.44$, $b_3 = 0.75$, $b_4 = 7.5$ and $T_0 = 270$ MeV.

The FRG flow equation for the thermodynamic potential in general contains mesons, quarks and Polyakov loops as dynamical fields. However, in the current calculation, we treat the Polyakov loop as a background field which is introduced self-consistently on the mean-field level. Following previous work [14, 30], we formulate the flow equation for the scale-dependent grand canonical thermodynamic potential density for quarks and mesons

$$\begin{aligned} \partial_k \Omega_k(\ell, \ell^*; T, \mu_q) = & \frac{k^4}{12\pi^2} \left\{ \frac{3}{E_\pi} \left[1 + 2n_B(E_\pi; T) \right] + \frac{1}{E_\sigma} \left[1 + 2n_B(E_\sigma; T) \right] \right. \\ & \left. - \frac{4N_c N_f}{E_q} \left[1 - N(\ell, \ell^*; T, \mu_q) - \bar{N}(\ell, \ell^*; T, \mu_q) \right] \right\}. \quad (23) \end{aligned}$$

Here

$$n_B(E_{\pi,\sigma}; T) = \frac{1}{\exp(E_{\pi,\sigma}/T) - 1}, \quad (24)$$

is the bosonic distribution function, with the pion and sigma energies,

$$E_\pi = \sqrt{k^2 + \overline{\Omega}'_k}, \quad E_\sigma = \sqrt{k^2 + \overline{\Omega}'_k + 2\rho \overline{\Omega}''_k}, \quad (25)$$

where $\overline{\Omega}_k = \Omega_k + c\sigma$ and primes denote the derivatives with respect to $\rho = \sigma^2/2$. The momentum distributions of quarks N and antiquarks \bar{N} are modified owing to the coupling to gluons,

$$\begin{aligned} N(\ell, \ell^*; T, \mu_q) &= \frac{1 + 2n_{\bar{q}}\ell^* + n_{\bar{q}}^2\ell}{1 + 3n_{\bar{q}}^2\ell + 3n_{\bar{q}}\ell^* + n_{\bar{q}}^3}, \\ \bar{N}(\ell, \ell^*; T, \mu_q) &= N(\ell^*, \ell; T, -\mu_q), \end{aligned} \quad (26)$$

where $E_q = \sqrt{k^2 + 2g^2\rho}$ is the quark energy and $n_{\bar{q}}(E_q; T, \mu_q) = \exp[\beta(E_q - \mu_q)]$.

We solve the flow equation for $\Omega_k(T, \mu_q)$ numerically by expanding it in powers of field variable, ρ , around the scale dependent potential minimum $\rho_k = \sigma_k^2/2$,

$$\bar{\Omega}_k(T, \mu_q) = \sum_{m=0}^M \frac{a_{m,k}(T, \mu_q)}{m!} (\rho - \rho_k)^m. \quad (27)$$

The location of the scale dependent minimum of thermodynamic potential $\Omega_k(T, \mu_q)$ is determined by the stationarity condition

$$\left. \frac{d\Omega_k}{d\sigma} \right|_{\sigma=\sigma_k} = \left. \frac{d\bar{\Omega}_k}{d\sigma} \right|_{\sigma=\sigma_k} - c = 0. \quad (28)$$

Truncating the expansion in Eq. (27) at $M = 3$, Eq. (23) yields the flow equation for the Taylor coefficients and field variable, ρ_k , as

$$\partial_k a_{0,k} = \frac{c}{\sqrt{2\rho_k}} \partial_k \rho_k + \partial_k \Omega_k, \quad (29)$$

$$\partial_k \rho_k = -\frac{1}{c/(2\rho_k)^{3/2} + a_{2,k}} \partial_k \Omega'_k, \quad (30)$$

$$\partial_k a_{2,k} = a_{3,k} \partial_k \rho_k + \partial_k \Omega''_k, \quad (31)$$

$$\partial_k a_{3,k} = \partial_k \Omega'''_k. \quad (32)$$

These differential equations are solved numerically with the initial cutoff $\Lambda = 1.2$ GeV (for details see Refs. [14, 30]). The initial conditions for the flow are chosen to reproduce the pion mass in vacuum $m_\pi = 138$ MeV, the pion decay constant $f_\pi = 93$ MeV, the sigma mass $m_\sigma = 600$ MeV and the constituent quark mass $m_q = 310$ MeV at the scale $k = 0$.

By construction, the solution of Eq. (23), Ω_k , computed at the minimum $\rho = \rho_k$ describes the scale-dependent thermodynamic potential density, where the contribution of soft quark and meson modes with $|\vec{q}| < k$ is suppressed [30]. Integrating the flow equation from $k = \Lambda$ to $k \rightarrow 0$, we obtain the thermodynamic potential which accounts for all momentum modes $|\vec{q}| < \Lambda$. The solution of equations (29-32), yields the thermodynamic potential density for quarks and mesons, $\Omega_{k \rightarrow 0}(\ell, \ell^*; T, \mu_q)$, as a function of the Polyakov loop variables ℓ and ℓ^* . The full thermodynamic potential density $\Omega(\ell, \ell^*; T, \mu_q)$ in the PQM model, including quarks, mesons and gluons, is

obtained by adding the effective gluon potential to $\Omega_{k \rightarrow 0}(\ell, \ell^*; T, \mu_q)$,

$$\Omega(\ell, \ell^*; T, \mu_q) = \Omega_{k \rightarrow 0}(\ell, \ell^*; T, \mu_q) + \mathcal{U}(\ell, \ell^*), \quad (33)$$

where at a given temperature and chemical potential, the Polyakov loop variables are determined by the stationarity conditions:

$$\frac{\partial}{\partial \ell} \Omega(\ell, \ell^*; T, \mu_q) = 0, \quad \frac{\partial}{\partial \ell^*} \Omega(\ell, \ell^*; T, \mu_q) = 0. \quad (34)$$

The thermodynamic potential (33) does not contain the contributions of statistical modes with momenta larger than the cutoff Λ . In order to obtain the correct high-temperature behavior of the thermodynamics we supplement the FRG potential with the contribution of high-momentum states with $|\vec{q}| > \Lambda$. This contribution to the flow is approximated by that of massless quarks interacting with the Polyakov loops [14, 30],

$$\begin{aligned} \partial_k \Omega_k^\Lambda(T, \mu_q) &= -\frac{N_c N_f k^3}{3\pi^2} \\ &\left[1 - N(\ell, \ell^*; T, \mu_q) - \bar{N}(\ell, \ell^*; T, \mu_q) \right]. \end{aligned} \quad (35)$$

The complete thermodynamic potential of the PQM model is then obtained by integrating Eq. (35) from $k = \infty$ to $k = \Lambda$, where we switch to the PQM flow equation (23). The thermodynamic potential thus obtained can be used to explore the properties of different cumulants of the net baryon number fluctuations.

The flow equation yields the thermodynamic potential as a function of temperature and chemical potential. Different cumulants of the net baryon number fluctuations χ_n^B , Eq. (5), can then in principle be obtained by explicit numerical differentiation. However, owing to the numerical errors accumulated in the solution of the flow equations, this method does not provide reliable results. Therefore, we compute the higher cumulants by analytically differentiating the flow equations (29-32) and (35) with respect to $\hat{\mu}_q$. This defines flow equations for χ_1^B and χ_2^B , which are solved using the solution of Eqs. (29-32) as input. Subsequently, the higher cumulants of the net baryon number fluctuations up to eighth order are computed by numerical differentiations of χ_2^B .

References

- [1] S. Jeon and V. Koch, in Quark Gluon Plasma 3. pp 430, Eds. R.C. Hwa and X. N. Wang, (World Scientific Publishing 2004).
- [2] M. A. Stephanov, Prog. Theor. Phys. Suppl. **153**, 139 (2004). Int. J. Mod. Phys. **A20**, 4387 (2005).
- [3] M. A. Stephanov, K. Rajagopal and E. V. Shuryak, Phys. Rev. Lett. **81**, 4816 (1998).
- [4] S. Ejiri, F. Karsch and K. Redlich, Phys. Lett. **B633**, 275-282 (2006).
- [5] M. A. Stephanov, Phys. Rev. Lett. **102**, 032301 (2009).
- [6] See e.g.: Proceedings of Quark Matter 2009, Nucl. Phys. **A830** (2009).
- [7] P. Braun-Munzinger, K. Redlich, and J. Stachel, in Quark-Gluon Plasma 3, Eds. R.C. Hwa and X.N. Wang, (World Scientific Publishing, 2004); A. Andronic, P. Braun-Munzinger, and J. Stachel, Acta Phys. Polon. **B40**, 1005 (2009).
- [8] P. Braun-Munzinger, J. Stachel, C. Wetterich, Phys. Lett. **B596**, 61 (2004).
- [9] O. Kaczmarek, F. Karsch, E. Laermann, C. Miao, S. Mukherjee, P. Petreczky, C. Schmidt, W. Soeldner and W. Unger, Phys. Rev. **D83**, 014504 (2011).
- [10] C.R. Allton, M. Doering, S. Ejiri, S.J. Hands, O. Kaczmarek, F. Karsch, E. Laermann and K. Redlich Phys. Rev. **D71**, 054508 (2005).
- [11] J. Engels, L. Fromme and M. Seniuch, Nucl. Phys. **B675**, 533 (2003).
- [12] R. V. Gavai and S. Gupta, Phys. Rev. **D78**, 114503 (2008).
- [13] M. Asakawa, S. Ejiri and M. Kitazawa, Phys. Rev. Lett. **103**, 262301 (2009).
- [14] V. Skokov, B. Friman and K. Redlich, arXiv:1008.4570 [hep-ph].
- [15] S. Ejiri, F. Karsch, E. Laermann, C. Miao, S. Mukherjee, P. Petreczky, C. Schmidt, W. Soeldner and W. Unger, Phys. Rev. **D80**, 094505 (2009).

- [16] J. Engels and F. Karsch, arXiv:1105.0584 [hep-lat].
- [17] G. Endrodi, Z. Fodor, S. D. Katz, K. K. Szabo, arXiv:1102.1356 [hep-lat].
- [18] for a summary of earlier results on the curvature of the transition line see: O. Philipsen, Prog. Theor. Phys. Suppl. **174**, 206 (2008).
- [19] A. Cucchieri, J. Engels, S. Holtmann, T. Mendes and T. Schulze, J. Phys. A: Math. Gen. **35**, 6517 (2002).
- [20] C. Schmidt, Prog. Theor. Phys. Suppl. **186**, 563-566 (2010).
- [21] K. Fukushima, Phys. Lett. **B591**, 277 (2004).
- [22] K. Fukushima, Phys. Lett. **B553**, 38 (2003);
K. Fukushima, Phys. Rev. **D68**, 045004 (2003).
- [23] C. Ratti, S. Roessner and W. Weise, Phys. Lett. **B649**, 57 (2007).
- [24] C. Sasaki, B. Friman, K. Redlich, Phys. Rev. **D75**, 074013 (2007).
- [25] B. J. Schaefer, J. M. Pawłowski and J. Wambach, Phys. Rev. **D76**, 074023 (2007).
- [26] C. Wetterich, Phys. Lett. **B301**, 90 (1993).
- [27] T. R. Morris, Int. J. Mod. Phys. **A9**, 2411 (1994).
- [28] U. Ellwanger, Z. Phys. **C62**, 503 (1994).
- [29] J. Berges, N. Tetradis and C. Wetterich, Phys. Rept. **363**, 223 (2002).
- [30] V. Skokov, B. Stokic, B. Friman and K. Redlich, Phys. Rev. **C82**, 015206 (2010).
- [31] B. Stokic, B. Friman, K. Redlich, Eur. Phys. J. **C67**, 425 (2010).
- [32] B. J. Schaefer, M. Wagner and J. Wambach, PoS **CPOD2009**, 017 (2009).
- [33] M. Cheng, P. Hegde, C. Jung, F. Karsch, O. Kaczmarek, E. Laermann, R. D. Mawhinney, C. Miao, P. Petreczky, C. Schmidt and W. Soeldner, Phys. Rev. **D79**, 074505 (2009).

- [34] W.-j. Fu, Y.-x. Liu and Y.-L. Wu, Phys. Rev. **D81**, 014028 (2010).
- [35] M. M. Aggarwal et al. (STAR Collaboration), Phys. Rev. Lett. **105**, 22302 (2010).
- [36] F. Karsch and K. Redlich, Phys. Lett. **B695**, 136 (2011).
- [37] R. V. Gavai and S. Gupta, Phys. Lett. **B696**, 459 (2011).